

# Influence of phase composition on the reentrant superconducting properties of $\text{Tm}_2\text{Fe}_3\text{Si}_5$

H. Schmidt, M. Müller, and H. F. Braun

*Physikalisches Institut, Universität Bayreuth, 95440 Bayreuth, Germany*

(Received 13 April 1995; revised manuscript received 30 October 1995)

The compound  $\text{Tm}_2\text{Fe}_3\text{Si}_5$  is the only known reentrant superconductor in which superconductivity is destroyed at the antiferromagnetic transition. Widely differing behavior has been reported in the literature regarding the occurrence of superconductivity ranging from transition temperatures around 1.7 K at atmospheric pressure to no superconductivity except under applied hydrostatic pressure. In order to clarify this situation, we carried out ac-susceptibility measurements under applied pressure and magnetization measurements as a function of phase composition within the homogeneity range of the compound and on multiphase samples. For single-phase samples,  $T_c$  decreases strongly in the whole pressure range with growing stoichiometric ratio Fe/Si. For multiphase samples, a shift of the  $T_c$  vs pressure curves to lower pressure values was observed. The high-temperature part of the susceptibility follows a Curie-Weiss law independent of phase composition which amounts to an effective magnetic moment per Tm atom of  $7.0\mu_B$ . With our results we are able to explain all the observed sample dependence of  $T_c$  with a combination of substitution effects in the homogeneity range of this compound and internal stress effects caused by impurity phases. [S0163-1829(96)06018-3]

## I. INTRODUCTION

The phenomenon of reentrant superconductivity, an interesting aspect of the interplay between superconductivity and long-range magnetic order, appears in several rare-earth (RE) compounds with a spatially ordered sublattice of RE atoms. In general, superconductivity is destroyed by ferromagnetic ordering, as, e.g., in  $\text{ErRh}_4\text{B}_4$  and  $\text{HoMo}_6\text{S}_8$ ,<sup>1</sup> while long-range antiferromagnetic ordering usually can coexist with superconductivity as, e.g., in  $\text{RRh}_4\text{B}_4$  ( $R = \text{Nd}, \text{Sm}, \text{Tm}$ ) and in a number of Chevrel-type RE compounds.<sup>1</sup> A recent example is the superconductor  $\text{HoNi}_2\text{B}_2\text{C}$  which nearly reenters the normal state when the Ho moments show a spiral magnetic ordering between 5 and 6 K, while at lower temperature a long-range ordered antiferromagnetic state coexists with superconductivity.<sup>2-6</sup>

In contrast,  $\text{Tm}_2\text{Fe}_3\text{Si}_5$  is the only known reentrant superconductor in which superconductivity is destroyed when the Tm moments order antiferromagnetically at about 1.1 K.<sup>7,8,14</sup> This noncoexistence is not understood at present. A detailed interpretation has been hampered by the apparent sample dependence of properties like, e.g., the observed transition temperature for superconductivity,  $T_c$ . Widely differing values ranging from onset temperatures for superconductivity of 1.7 K at atmospheric pressure<sup>7</sup> up to the observation that no superconducting transition occurs without applied pressure<sup>15</sup> were reported in the literature.

$\text{Tm}_2\text{Fe}_3\text{Si}_5$  crystallizes in the  $\text{Sc}_2\text{Fe}_3\text{Si}_5$  structure with tetragonal space group  $P4/mnc$  and lattice parameters of  $a = 10.37(1) \text{ \AA}$  and  $c = 5.405(1) \text{ \AA}$ .<sup>9</sup> Mössbauer studies show that in the structure series  $\text{R}_2\text{Fe}_3\text{Si}_5$  ( $R = \text{rare earths}$ ) the upper limit for a magnetic moment on the Fe sites is smaller than  $0.07\mu_B$  due to covalent bonding with silicon.<sup>10-13</sup> The Fe  $3d$  electrons appear to be responsible for the occurrence of the superconducting state<sup>10</sup> while the antiferromagnetic structure is formed by a noncollinear alignment of the  $\text{Tm}^{3+}$  magnetic moments in the basal plane.<sup>14,8</sup>

Beside its interesting magnetic and superconducting prop-

erties,  $\text{Tm}_2\text{Fe}_3\text{Si}_5$  shows an amazing behavior under applied hydrostatic pressure.<sup>15</sup> Up to 20 kbar a nonlinear dependence of  $T_c$  on pressure with a maximum of about 3.13 K at 9 kbar and one of the largest known positive pressure derivatives  $dT_c/dp = 0.47 \text{ K/kbar}$  are observed. In contrast, the value of the reentrant temperature corresponding to the Néel temperature  $T_N = 1.15 \text{ K}$  is relatively independent of pressure.<sup>15</sup> Neutron diffraction measurements show that the antiferromagnetic structure is unchanged under applied pressure.<sup>8</sup>

The physical properties of a sample, like the superconducting and magnetic transition temperatures, phononic and electronic properties, the lattice parameters, and the volume of the unit cell, are determined by its thermodynamic state, described by appropriate variables. One of these variables is the phase composition, meaning the concentration of the elements in a single-phase material. In this paper, we present a detailed study of the superconductivity in  $\text{Tm}_2\text{Fe}_3\text{Si}_5$  as a function of phase composition in single-phase samples, as well as in multiphase samples. This study permits one to distinguish between composition-dependent phase properties of  $\text{Tm}_2\text{Fe}_3\text{Si}_5$  and behavior induced by impurity phases due to strain effects. High-temperature susceptibility studies indicate that excess iron does not carry a magnetic moment, virtually excluding addition magnetic pair breaking as the reason for the decrease of  $T_c$  with increasing Fe/Si ratio.

## II. SAMPLE PREPARATION AND EXPERIMENTAL DETAILS

All samples were prepared from high-purity elements (Tm, 99.9%; Fe, 99.999%; and Si, 99.999%) melted together in an arc furnace under Ar atmosphere. The resulting ingots were turned over 5 times and remelted to promote homogeneity. The maximum losses during melting of about 2% of the sample mass were due to evaporation of pure Tm, and splintering off of small amounts of material with unknown composition from the inhomogeneous sample during cooling on the copper hearth. The samples were sealed in quartz cap-

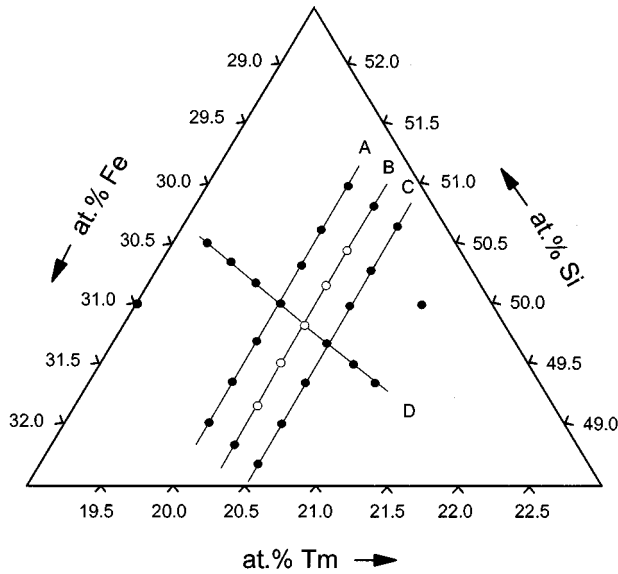
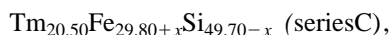
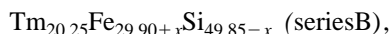
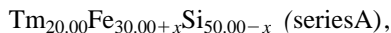


FIG. 1. Nominal composition of the prepared samples, displayed in a partial isothermal section at 800 °C:  $\text{Tm}_{20.00}\text{Fe}_{30.00+x}\text{Si}_{50.00-x}$  (series A),  $\text{Tm}_{20.25}\text{Fe}_{29.90+x}\text{Si}_{49.85-x}$  (series B),  $\text{Tm}_{20.50}\text{Fe}_{29.80+x}\text{Si}_{49.70-x}$  (series C),  $x=0, \pm 0.30, \pm 0.60, \pm 1.00$ ,  $\text{Tm}_{20.00+x}\text{Fe}_{30}\text{Si}_{50}$  (series D),  $x=0, \pm 0.30, \pm 0.62, \pm 0.92, 1.23$ ; solid circle, multiphase samples; open circle, single-phase sample or sample with very minor impurity phase; the stoichiometric composition is at the crossing of series A and D.

sules under 300 mbar Ar, heat treated for 2 days at 1100 °C, 2 days at 1000 °C, and 4 days at 800 °C, and then quenched in water. This heat treatment procedure was chosen as a compromise between preparation time and sample homogeneity. As it turned out, sample homogeneity could be improved by prolonged heating at 1100 °C (21 days) followed by the 1000 and 800 °C equilibration steps.

Due to the mass losses of 2%, a well-defined phase composition could not be reached by melting individual phase samples from the elements. Therefore, samples with defined relative distance in composition diagram were made by first producing two master alloys. The uncertainty of the absolute sample position in composition space is about 0.4 at.%, whereas that in relative position between samples of the same series is about 0.05 at.%. Starting with four pairs of master alloys, four series of samples were prepared (Fig. 1), three at constant Tm concentration



$x=0, \pm 0.30, \pm 0.60, \pm 1.00$ , and one at fixed stoichiometric ratio Fe/Si  $\text{Tm}_{20.00+x}\text{Fe}_{30}\text{Si}_{50}$  (series D),  $x=0, \pm 0.30, \pm 0.62, \pm 0.92, 1.23$ . In addition, some samples were prepared individually.

Phase analysis was performed by x-ray powder diffraction on a Seifert XRD 3000 P diffractometer with secondary monochromator, using Cu  $K\alpha$  radiation. Lattice parameters were refined with the method of least squares. In addition to

an analysis of the x-ray intensities, optical metallography, and energy dispersive x-ray analysis (EDX) measurements on a Jeol JSM-840 electron microscope were used to estimate the amount and kind of impurities in the samples.

The superconducting and magnetic transitions were detected by ac-susceptibility measurements at 20 Hz and 1 Oe. The transition temperature was defined at 50% of the full signal change. The applied pressure was produced by a standard CuBe piston-cylinder technique with Sn as superconducting manometer. Magnetization measurements at standard pressure were carried out on a Cryogenics S 600 superconducting quantum interference device (SQUID) magnetometer from 2 to 300 K. For these measurements, the samples were ground into spheres and corresponding demagnetization corrections were applied.

### III. RESULTS AND DISCUSSION

#### A. Phase analysis

$\text{Tm}_2\text{Fe}_3\text{Si}_5$  is in equilibrium with  $\text{TmFe}_2\text{Si}_2$ ,  $\text{TmSi}$ , and  $\text{FeSi}$  and three phases with nominal composition  $\text{Tm}_9\text{Fe}_{26}\text{Si}_{65}$ ,  $\text{Tm}_{21.0}\text{Fe}_{18.5}\text{Si}_{60.5}$ , and  $\text{Tm}_{30.0}\text{Fe}_{12.8}\text{Si}_{57.2}$ . Details of the phase diagram are planned to be published elsewhere.<sup>16</sup> The sample series  $\text{Tm}_{20.25}\text{Fe}_{29.90+x}\text{Si}_{49.85-x}$  (series B), which showed the lowest amount of impurity phases, and series  $\text{Tm}_{20.00+x}\text{Fe}_{30}\text{Si}_{50}$  (series D) with changing Tm concentration got an additional thermal treatment for 21 days at 1100 °C, 2 days at 1000 °C and 4 days at 800 °C in order to further improve sample homogeneity. This way, samples with no or very minor detectable impurity phases in the x-ray diffraction (XRD) patterns could be produced. The size of the homogeneity range was determined from these samples. The extent is very small, approximately 1–2 at.% along fixed Tm concentration and smaller than 0.3 at.% along varying Tm concentration. “ $\text{Tm}_2\text{Fe}_3\text{Si}_5$ ” is not a stoichiometric compound, since the 2:3:5 composition corresponds only to a point in the homogeneity domain in the isothermal section of the ternary diagram. The stoichiometric 2:3:5 composition in Fig. 1 is at the crossing of lines A and D, while single-phase samples have been found in series B only. We stress that nominal composition is plotted in Fig. 1, and not the sample composition which we estimate to be uncertain by about 0.4 at.% as discussed in Sec. II above. Thus, it is not excluded that the homogeneity domain of the phase “ $\text{Tm}_2\text{Fe}_3\text{Si}_5$ ” contains the stoichiometric composition. Considering the evaporation losses of Tm during melting it is in fact quite likely that the true Tm content of series B corresponds to the stoichiometric amount. Phases with a fixed content of rare earth combined with a variable ratio of transition metal to main group element, usually described by stoichiometric structure types, are not uncommon in ternary rare-earth–transition-metal–silicon systems.<sup>17</sup>

With the variation of phase composition in the homogeneity range one can assume that vacancy formation or mutual substitution of the atoms involved, Fe and Si, takes place. This can affect the lattice parameters if the involved atoms have different size. A change in the lattice parameters may lead to a volume change of the unit cell and could influence the superconducting properties of the compound in the same way as applied pressure. However, the refinement of the lattice constants of all samples revealed, within error limits, no

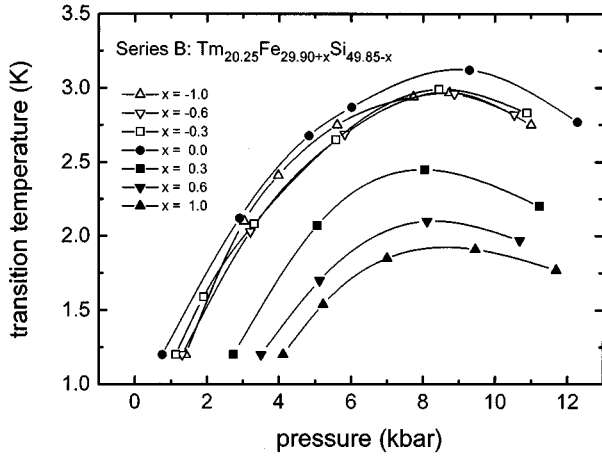


FIG. 2. Pressure dependence of the superconducting transition midpoint temperature for nominal composition  $\text{Tm}_{20.25}\text{Fe}_{29.90+x}\text{Si}_{49.85-x}$  (series B).

significant variation. We obtain  $a = 10.367(1) \text{ \AA}$  and  $c = 5.407(1) \text{ \AA}$  in good agreement with the literature.<sup>9</sup>

### B. ac-susceptibility measurements

For the post-annealed sample series B and D, ac-susceptibility measurements under hydrostatic pressure were performed to determine the composition dependence of the superconducting and magnetic transitions. The results are shown in Figs. 2 and 3. All curves show typical nonlinear behavior with a broad maximum around 9 kbar. None of the samples is fully superconducting at ambient pressure above the reentrant temperature of 1.15 K; only a slight onset of a few percent of the full diamagnetic signal is found in some samples. For clarity, we do not include in the figures the reentrant transition temperature, also measured by ac susceptibility. We find that this reentrant temperature, which coincides with the Néel temperature  $T_N$  indicating the transition to antiferromagnetic order,<sup>8,14</sup> is nearly independent of phase composition and shows only a weak shift to higher temperatures of at most 30 mK with increasing iron content.

The  $T_c$  vs pressure curves for the different samples of series B, denoted as  $\text{Tm}_{20.25}\text{Fe}_{29.90+x}\text{Si}_{49.85-x}$ , clearly show that for the nominally Si-rich samples there is only a weak variation in  $T_c$  (Fig. 2). In contrast, for the nominally Fe-rich samples, a rapid decrease in  $T_c$  occurs over the full pressure range with growing Fe content. For the samples with a superconducting midpoint below 1.7 K,  $T_c$  was extrapolated from the expected full throw of the signal. The maximum  $T_c$  of 3.2 K at 9 kbar for  $\text{Tm}_{20.25}\text{Fe}_{29.90}\text{Si}_{49.85}$  ( $x=0$ ) is shifted to 1.95 K for sample  $\text{Tm}_{20.25}\text{Fe}_{30.90}\text{Si}_{48.85}$  ( $x=1.0$ ) (Fig. 2). The maximum pressure coefficient  $dT_c/dp$  was determined to about  $0.5 \pm 0.05 \text{ K/kbar}$ . No systematic variation with composition is observed for the pressure coefficient at constant pressure.

In contrast to series B, the analysis of sample series  $\text{Tm}_{20.00+x}\text{Fe}_{30}\text{Si}_{50}$  (series D) shows no obvious variation of the  $T_c$  vs pressure curves with changing nominal concentration of the rare earth (Fig. 3). This can be explained with a vanishing extent of the homogeneity range along changing

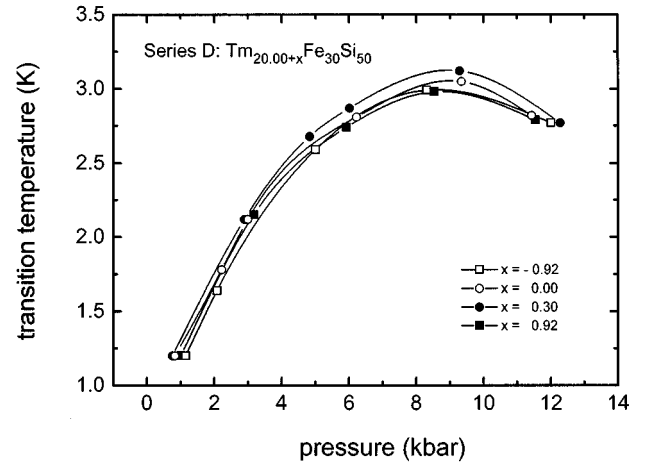


FIG. 3. Pressure dependence of the superconducting transition midpoint temperature for nominal composition  $\text{Tm}_{20.00+x}\text{Fe}_{30}\text{Si}_{50}$  (series D).

Tm concentration. All samples would have the same phase composition of the  $\text{Tm}_2\text{Fe}_3\text{Si}_5$  phase.

The decrease of  $T_c$  with overstoichiometric Fe content is clearly seen in Fig. 4. At any given Fe concentration, the  $T_c$  depression is independent of pressure. This means that the  $T_c$  vs pressure curves in Fig. 2 are shifted parallel to the temperature axis with increasing Fe/Si ratio. We note that in contrast to binary systems, no straightforward conclusion concerning the boundaries of the homogeneity domain can be drawn from variation or constancy of  $T_c$  as a function of composition in a ternary system.

The reason for the  $T_c$  depression with increasing Fe content could be magnetic pair breaking due to a residual moment of Fe atoms substituting on Si sites. Such substitution does not necessarily affect the lattice parameters since the metallic radii of Si (1.17 Å) and Fe (1.24 Å) are similar. Incorporated additional Fe atoms may keep a residual magnetic moment due to changed bonding conditions and can

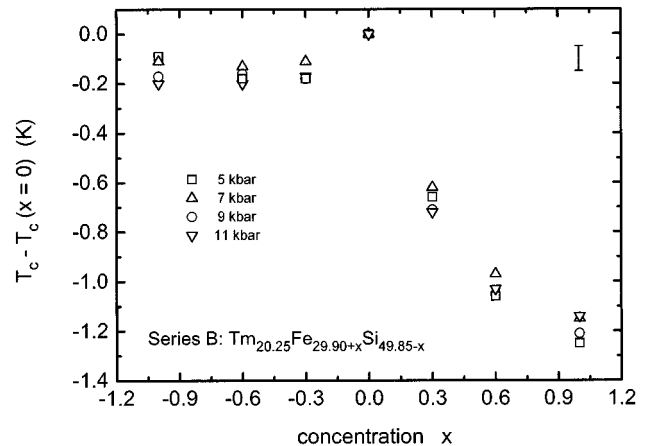


FIG. 4. Variation of the superconducting transition temperature with phase composition at different pressures for nominal composition  $\text{Tm}_{20.25}\text{Fe}_{29.90+x}\text{Si}_{49.85-x}$  (series B); the bar denotes the typical error.

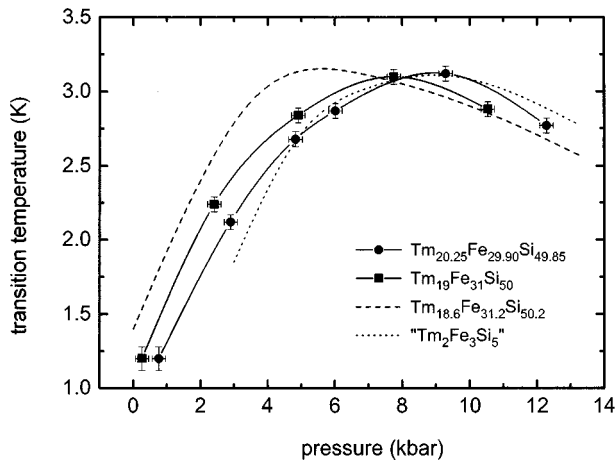


FIG. 5. Comparison of  $T_c$  vs pressure curves with literature data:  $\text{Tm}_{20.25}\text{Fe}_{29.90}\text{Si}_{49.85}$  (single phase, series B),  $\text{Tm}_{19.00}\text{Fe}_{31.00}\text{Si}_{50.00}$  (multiphase, individually prepared),  $\text{Tm}_{18.6}\text{Fe}_{31.2}\text{Si}_{50.2}$  [multiphase (Ref. 18)], and  $\text{Tm}_2\text{Fe}_3\text{Si}_5$  [single phase (Ref. 15)].

appear as magnetic impurities. In this case, the lowering of  $T_c$  may be explained by magnetic pair breaking. A different explanation takes into account that the nonlinear pressure behavior of  $T_c$  can be seen as the effect of the Fermi-level sweeping through a peak in the density of states with increasing pressure, as suggested by Segre for the pressure behavior of  $\text{Y}_2\text{Fe}_3\text{Si}_5$ .<sup>19</sup> The decrease of the transition temperature with increasing Fe content is then the result of a disorder-induced broadening of the peak and a decrease of the maximum in the density of states.

In addition to the four series, some samples not prepared from master alloys were measured. The  $T_c$  vs pressure curve of the sample with nominal composition  $\text{Tm}_{19}\text{Fe}_{31}\text{Si}_{50}$ , as a typical example, appears shifted along the pressure axis by 0.5 kbar to lower pressures, as compared to  $\text{Tm}_{20.25}\text{Fe}_{29.90}\text{Si}_{49.85}$  (series B), but shows no decrease of the maximum  $T_c$  (Fig. 5). In a similar way, the pressure curve reported by Braun<sup>18</sup> on a sample with nominal composition  $\text{Tm}_{18.6}\text{Fe}_{31.2}\text{Si}_{50.2}$  and a different heat treatment of 2 days at 1200 °C and 2 days at 1000 °C appears shifted by 1 kbar to lower pressures. The curve presented by Vining and Shelton<sup>15</sup> appears to be shifted to slightly higher pressures.

Our samples that show this shift parallel to the pressure axis are not single phase. It is possible that one or more impurity phases present in the sample have a coefficient of thermal expansion different from that of  $\text{Tm}_2\text{Fe}_3\text{Si}_5$ . Thus an ‘‘internal’’ stress could be produced when the samples are cooled from the melting point on the copper hearth or later, during cooling from room temperature to the kelvin range. This internal pressure effect is not necessarily visible in a significant change of the unit cell volume. If we assume a volume of the unit cell of  $V = 581.1(6) \text{ \AA}^3$ , a compressibility of  $\kappa = 10^{-4} - 10^{-3} \text{ kbar}^{-1}$  as estimated by Segre,<sup>19</sup> and the maximum observed shift on the pressure scale as  $\Delta p = 1 \text{ kbar}$ , we obtain a volume change of the unit cell of  $\Delta V = V\kappa\Delta p \approx 0.06 - 0.6 \text{ \AA}^3$ , which is within the estimated errors of volume determination. Note that this internal effect is due to the multiphase nature of a given sample and not

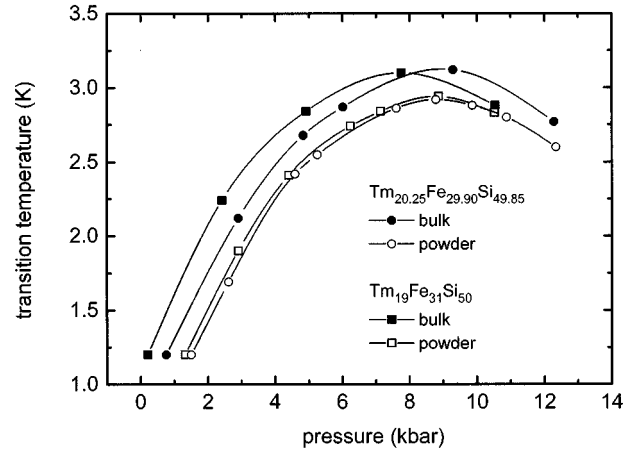


FIG. 6. Superconducting transition temperature  $T_c$  as a function of pressure for bulk samples and ground and strain-release annealed powder for nominal composition  $\text{Tm}_{20.25}\text{Fe}_{29.90}\text{Si}_{49.85}$  (single phase, series B) and  $\text{Tm}_{19.00}\text{Fe}_{31.00}\text{Si}_{50.00}$  (multiphase, individually prepared).

intrinsic to the  $\text{Tm}_2\text{Fe}_3\text{Si}_5$  phase, as would be, e.g., a ‘‘chemical pressure effect’’ due to substitutional dissolution in the crystallographic lattice of an atomic species of larger atomic volume. The steep pressure gradient of  $T_c$  is, however, intrinsic to the  $\text{Tm}_2\text{Fe}_3\text{Si}_5$  phase.

In order to test whether the shift in the measured curves is indeed caused by ‘‘internal’’ pressure effects, the samples with nominal composition  $\text{Tm}_{20.25}\text{Fe}_{29.90}\text{Si}_{49.85}$  (series B) and  $\text{Tm}_{19}\text{Fe}_{31}\text{Si}_{50}$  were carefully ground to a grain size of 50–500  $\mu\text{m}$ , heat treated for 1 day at 800 °C to release strains, and then  $T_c$  was determined again. The essential differences between the two samples have disappeared, as shown in Fig. 6. This result demonstrates that internal pressure effects play an important role in determining the superconducting transition temperature even at ambient pressure. Given the different heat treatments and sample compositions used by different groups<sup>7,15,18</sup> the fact that superconductivity is sometimes found in this system at ambient pressure can easily be explained.

### C. Magnetization measurements

In order to examine whether the excess iron carries a magnetic moment, all samples of series  $\text{Tm}_{20.25}\text{Fe}_{29.90+x}\text{Si}_{49.85-x}$  (series B) were investigated in a field of 100 Oe in a commercial SQUID magnetometer with a useful temperature range down to about 2 K. As an example for the whole series the inverse mass susceptibility is plotted as a function of temperature for  $\text{Tm}_{20.25}\text{Fe}_{30.20}\text{Si}_{49.55}$  ( $x = -0.30$ ) in Fig. 7. The high temperature susceptibility ( $T > 70 \text{ K}$ ) of all samples can be fitted with a Curie-Weiss law:

$$\chi = \chi_0 + \frac{C}{T - \Theta},$$

where  $C$  is the Curie constant,  $\Theta$  the paramagnetic Curie temperature, and  $\chi_0$  the temperature-independent contribution to the susceptibility, caused by ion cores and the con-

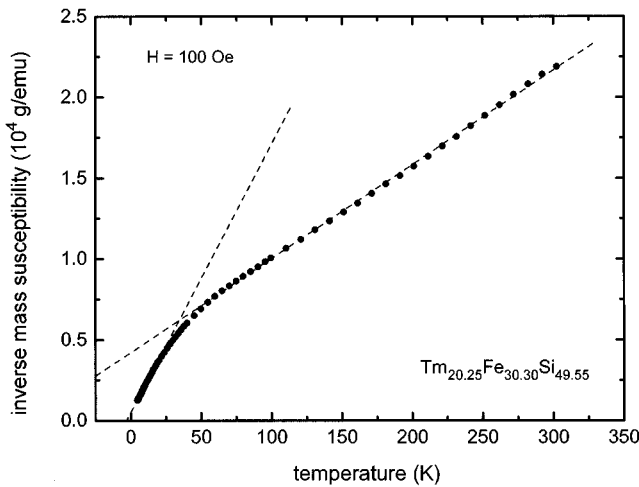


FIG. 7. Inverse mass susceptibility  $H/M$  as a function of temperature at 100 Oe for  $\text{Tm}_{20.25}\text{Fe}_{30.30}\text{Si}_{49.55}$  (series B). Dotted lines are Curie-Weiss fits for the low- and high-temperature parts.

ducting electrons.  $\chi_0$  is of the order of  $10^{-6}$  emu/g and is negligible compared to  $\chi$ . The Curie constant shows no systematic variation with the Fe/Si ratio. The averaged effective magnetic moment per  $\text{Tm}^{3+}$  ion determined from the Curie constant is  $(7.0 \pm 0.3)\mu_B$ , which within errors equals the free ion value of  $7.3\mu_B$ .

Below 70 K the inverse susceptibility deviates from the Curie-Weiss behavior. This can be attributed to crystalline electric field (CEF) effects. A Curie-Weiss fit in that range results in a strongly different value for the averaged effective magnetic moment of  $(4.8 \pm 1.3)\mu_B$ . Since our samples are polycrystalline with an orientation distribution of the crystallites that is neither random nor fully textured, we refrain from an analysis in terms of CEF states.

The analysis of the SQUID measurements on samples with different phase compositions reveals no dependence of the Curie constant on Fe content. Covalent bonding with Si is thought to be responsible for the nonmagnetic nature of iron<sup>10–13</sup> in the  $R_2\text{Fe}_3\text{Si}_5$  series of compounds. The disorder introduced by the incorporation of excess iron, most likely on Si sites, then conceivably could lead to magnetic behavior of the iron.

However, the present results indicate that there is no significant change in the nonmagnetic nature of Fe in this compound. Thus, it appears unlikely that the depression of  $T_c$  in samples with higher than stoichiometric Fe/Si ratio is due to magnetic pair breaking caused by iron. Clearly, further investigations with more sensitive methods like Mössbauer measurements on the sample series with varying Fe content are indicated.

#### IV. SUMMARY

We used ac-susceptibility measurements under ambient and applied hydrostatic pressure as well as magnetization measurements to study the dependence of the superconducting and magnetic transition temperatures on phase composition in the homogeneity range of the ternary antiferromagnetic reentrant superconductor  $\text{Tm}_2\text{Fe}_3\text{Si}_5$ . The results on single-phase samples reveal that the superconducting transition temperature  $T_c$  is very sensitive to the stoichiometric ratio Fe/Si over the whole pressure range, while the antiferromagnetic transition temperature  $T_N$  remains nearly unchanged. This behavior is consistent with the incorporation of small amounts of magnetic iron as additional pair-breaking source. However, the high-temperature Curie constant is independent of the Fe/Si ratio and compatible with the free ion moment of trivalent Tm, indicating that there is no significant change in the nonmagnetic nature of iron in this compound. The analysis of multiphase samples reveals a shift of the pressure vs  $T_c$  curves to lower pressure values. This can be explained with internal stress effects, caused by different thermal expansions of matrix and impurity phases. With our measurements, it is possible to explain the observed sample dependence of  $T_c$  and provide an explanation for the different published<sup>7,18</sup> onset temperatures. In multiphase samples, due to the steep pressure gradient of  $T_c$ , internal strain effects caused by the impurity phases may induce superconductivity even at atmospheric pressure.

#### ACKNOWLEDGMENTS

EDX and scanning electron microscopy (SEM) measurements have been performed at the BIMF (Bayreuther Institut für Makromolekülforschung). We thank W. Ettig for technical support and C. Drummer for her assistance in EDX analysis.

<sup>1</sup>See, e.g., *Superconductivity in Ternary Compounds II*, edited by M.B. Maple and Ø. Fischer (Springer, Berlin, 1982).

<sup>2</sup>H. Eisaki, H. Takagi, R.J. Cava, K. Mizuhashi, J.O. Lee, B. Batlogg, J.J. Krajewski, W.F. Beck, Jr., and S. Uchida, *Phys. Rev. B* **50**, 647 (1994).

<sup>3</sup>H. Schmidt and H.F. Braun, *Physica C* **229**, 315 (1994).

<sup>4</sup>T.E. Grigereit, J.W. Lynn, Q. Huang, A. Santoro, R.J. Cava, J.J. Krajewski, and W.F. Peck, Jr., *Phys. Rev. Lett.* **73**, 2756 (1994).

<sup>5</sup>A.I. Goldman, C. Stassis, P.C. Canfield, J. Zarestky, P. Devenagas, B.K. Cho, and D.C. Johnston, *Phys. Rev. B* **50**, 9668 (1994).

<sup>6</sup>H. Schmidt, M. Weber, and H.F. Braun, *Physica C* **246**, 177 (1995).

<sup>7</sup>C.U. Segre and H.F. Braun, *Phys. Lett.* **85A**, 372 (1981).

<sup>8</sup>J.A. Gotaas, J.W. Lynn, R.N. Shelton, P. Klavins, and H.F. Braun, *Phys. Rev. B* **36**, 7277 (1987).

<sup>9</sup>D.C. Johnston and H.F. Braun, in *Superconductivity in Ternary Compounds II*, edited by M.B. Maple and Ø. Fischer (Springer, Berlin, 1982), p. 11.

<sup>10</sup>H.F. Braun, C.U. Segre, F. Acker, M. Rosenberg, and P. Deppe, *J. Magn. Magn. Mater.* **25**, 117 (1981).

<sup>11</sup>J.D. Cashion, G.K. Shenoy, D. Niarchos, P.J. Viccaro, and C.M. Falco, *Phys. Lett.* **79A**, 454 (1980).

<sup>12</sup>J.D. Cashion, G.K. Shenoy, D. Niarchos, P.J. Viccaro, A.D. Aldred, and C.M. Falco, *J. Appl. Phys.* **52**, 2180 (1981).

<sup>13</sup>D.R. Noakes, G.K. Shenoy, D. Niarchos, A.M. Umarji, and A.D.

- Aldred, Phys. Rev. B **27**, 4317 (1983).
- <sup>14</sup>A.R. Moodenbaugh, D.E. Cox, and C.B. Vining, Phys. Rev. B **32**, 3103 (1985).
- <sup>15</sup>C.B. Vining and R.N. Shelton, Solid State Commun. **54**, 53 (1985).
- <sup>16</sup>M. Müller, H. Schmidt, and H.F. Braun (unpublished).
- <sup>17</sup>See, e.g., E. Parthé and P. Chabot, in *Handbook on the Physics and Chemistry of Rare Earths*, edited by K.A. Gschneidner, Jr. and L.R. Eyring (North-Holland, Amsterdam, 1984), Vol. 6.
- <sup>18</sup>H.F. Braun, habilitation thesis, Université de Genève, 1986.
- <sup>19</sup>C.U. Segre, Ph.D. thesis, University of California at San Diego, 1981.